

## **Invader probes: Harnessing the energy of intercalation to facilitate recognition of chromosomal DNA for diagnostic applications**

Dale C. Guenther, Grace H. Anderson, Saswata Karmakar, Brooke A. Anderson, Bradley A. Didion, Wei Guo, John P. Versteegen and Patrick J. Hrdlicka.

### **Electronic supplementary information**

#### **Table of Contents**

Protocol - synthesis and purification of ONs	S3
Protocol - thermal denaturation experiments	S4
Protocol - determination of thermodynamic parameters	S4
Protocol - electrophoretic mobility shift assay	S4
Protocol - verification of gender via PCR	S5
Protocol - cell culture and nuclei preparation	S6
Protocol - fluorescence in situ hybridization	S6
Definition - interstrand zipper arrangement	S8
MALDI-MS of:	
ONs modified with 2'- <i>O</i> -(pyren-1-yl)methyl-RNA monomers (Table S1)	S9
ONs modified with 2'- <i>N</i> -(pyren-1-ylmethyl)-2'- <i>N</i> -methylamino-uridine monomers (Table S2)	S10
Representative thermal denaturation curves (Figure S1)	S11
Thermal denaturation temperatures and thermal advantages for other zipper interstrand zipper probes:	
X-modified ONs (Table S3)	S12
Y-modified ONs (Table S4)	S13
X- and A-modified ONs (Table S5)	S14
Thermodynamic parameters of hybridization for 13-mer duplexes	
Change in Gibbs free energy	
X-modified ONs (Table S6)	S15

<b>Y</b> -modified ONs (Table S7)	S16
Change in enthalpy	
<b>X</b> -modified ONs (Table S8)	S17
<b>Y</b> -modified ONs (Table S9)	S18
Graph of reaction enthalpy change (Figure S2)	S19
Change in entropy	
<b>X</b> -modified ONs (Table S10)	S20
<b>Y</b> -modified ONs (Table S11)	S21
Graph of reaction entropy change (Figure S3)	S22
Representative electrophoretograms of EMSA (Figure S4)	S23
Recognition of <b>DH1</b> or <b>DH8</b> - influence of loop orientation (Figure S5)	S24
Recognition of <b>DH1</b> using individual probe strands (Figure S6)	S25
Pseudo-first order kinetic profiles (Figure S7)	S26
Thermal denaturation temperatures of DNA hairpins (Table S12)	S27
Thermodynamic parameters of hybridization of ONs used in FISH assay:	
Change in Gibbs free energy (Table S13)	S28
Change in enthalpy (Table S14)	S29
Change in entropy (Table S15)	S29
Electrophoretogram of gender-specific PCR amplicons (Figure S8)	S30
Images using PNA as nd-FISH probes (Figure S9)	S31
Additional images from nd-FISH experiments using Invader probes (Figure S10)	S32
Images from nd-FISH control experiments (Figure S11)	S33
References	S34

**Protocol - synthesis and purification of ONs.** X/Y-modified ONs were synthesized on an automated DNA synthesizer (0.2  $\mu$ mol scale) using a long chain alkyl amine controlled pore glass (LCAA-CPG) solid support with a pore size of 500 Å. The corresponding phosphoramidites of monomers X and Y were prepared as previously described<sup>S1</sup> and incorporated into ONs via hand-couplings (0.05 M in acetonitrile, using 0.01 M 4,5-dicyanoimidazole or 5-ethylthio-1*H*-tetrazole as the activators (15 min) for A/C/X-modified or Y-modified ONs, respectively) with extended oxidation (45 s). Treatment with 32% ammonia (55 °C, 17 h) facilitated deprotection and cleavage from solid support. DMT-protected ONs were purified via ion-pair reverse phase HPLC (XTerra MS C18 column: 0.05 M triethyl ammonium acetate and acetonitrile gradient) followed by detritylation (80% acetic acid, 20 min) and precipitation (NaOAc, NaClO<sub>4</sub>, acetone, -18 °C, 16 h). The purity and identity of synthesized ONs were verified using analytical HPLC (>85% purity) and MALDI-MS analysis (Tables S1 and S2) recorded on a Quadrupole Time-of-Flight (Q-TOF) mass spectrometer with anthranilic acid or 3-hydroxypicolinic acid matrix for X- or Y-modified ONs, respectively.

Cy3-labeled X-modified ONs were synthesized as described above with the following modifications. After the incorporation of the last nucleotide, a C6-amino-modifier (Glen Research) was incorporated via hand coupling (4,5-dicyanoimidazole, 15 min, anhydrous CH<sub>3</sub>CN). The resulting ONs were worked up, purified, detritylated (glacial AcOH, 45 min, rt) and precipitated essentially as described above. The resulting amine-terminated ONs were dissolved in nanopure water, quantified, evaporated to dryness on a speedvac, dissolved in a minimum volume of water, and coupled with Cy3-*N*-hydroxysuccinimide ester (Lumiprobe, LLC) in DMSO as recommended by the vendor. Cy3-labeled ONs were precipitated twice from ethanol (0 °C for ~3h) and purified by RP-HPLC as described above.

**Protocol - thermal denaturation experiments.** The concentrations of ONs were estimated using the following extinction coefficients ( $OD_{260}/\mu\text{mol}$ ): G (12.01), A (15.20), T (8.40), C (7.05), pyrene (22.4) and Cy3 (4.93).<sup>S2</sup> Thermal denaturation temperatures were calculated as the first-derivative maximum of the  $A_{260}$  vs.  $T$  curve. ONs (1.0  $\mu\text{M}$ ) were annealed (85 °C for 2 min) in medium salt buffer ( $[\text{Na}^+] = 110 \text{ mM}$ ,  $[\text{Cl}^-] = 100 \text{ mM}$ , pH 7.0 ( $\text{NaH}_2\text{PO}_4/\text{Na}_2\text{HPO}_4$ ),  $[\text{EDTA}] = 0.2 \text{ mM}$ ) and subsequent cooling to the starting temperature. The experimental temperature ranged from at least 15 °C below  $T_m$  to 15 °C above  $T_m$ , with the  $T_m$  being determined as the average of two experiments within  $\pm 1.0$  °C.

**Protocol - determination of thermodynamic parameters.** Thermodynamic parameters for duplex formation were determined through baseline fitting of denaturation curves (van't Hoff method) using software with the UV-Vis spectrophotometer. Bimolecular reactions, two-state melting behavior, and constant heat capacity were assumed.<sup>S3</sup> Two curves per experiment were analyzed at least three times to minimize errors arising from baseline choice.

**Protocol - electrophoretic mobility shift assay.** DNA hairpins (DH) were obtained from commercial sources and used without further purification. Hairpins were labeled using the 2<sup>nd</sup> generation DIG Gel Shift Kit (Roche Applied Bioscience). Briefly, 11-digoxigenin-ddUTP was incorporated at the 3'-end of the hairpin (100 pmol) using a recombinant terminal transferase. The reaction mixture was quenched through addition of EDTA (0.05 M), diluted to 68.8 nM, and used without further processing. The recognition experiments were conducted essentially as previously reported.<sup>S4</sup> Thus, Invader probes (variable concentration) were annealed (90 °C for 2 min, followed by cooling to room temperature) and subsequently incubated with DIG-labeled DNA hairpins (34.4 nM) in HEPES buffer (50 mM HEPES, 100 mM NaCl, 5 mM  $\text{MgCl}_2$ , pH

7.2, 10% sucrose, 1.44 mM spermine tetrahydrochloride) at room temperature (~21 °C) for a specified period. Loading dye (6X) was added and the reaction mixtures were loaded onto 12% non-denaturing TBE-PAGE (45 mM tris-borate, 1 mM EDTA; acrylamide:bisacrylamide (19:1)). Electrophoresis was performed using constant voltage (70 V) at ~4 °C for 1.5 h. Bands were blotted onto positively charged nylon membranes (100 V, 30 min, ~4 °C) and cross-linked through exposure to UV (254 nm, 5 × 15 watt bulbs, 3 min). Membranes were incubated with anti-digoxigenin-alkaline phosphatase F<sub>ab</sub> fragments as recommended by manufacturer, and transferred to a hybridization jacket. Membranes were incubated with the chemiluminescence substrate (CSPD) for 10 min at 37 °C, and chemiluminescence was captured on X-ray films. Digital images of developed X-ray films were obtained using a Fluor-S MultiImager and quantified using appropriate software (Quantity One). The percentage of dsDNA recognition was calculated as the intensity ratio between the recognition complex band and the total lane. An average of three independent experiments is reported along with standard deviations (±).

**Protocol - verification of gender via PCR.** The gender of the somatic cell lines was confirmed via PCR as previously reported,<sup>S5</sup> using primers that specifically target bovine *ZFX* and *ZFY* gene sequences located on the X and Y chromosomes, respectively. The presence of a single band is indicative of a female, while two bands signal a male (Figure S7). Multiplex PCR (MJ Research PTC-200 thermocycler) was performed using the following protocol: 95 °C pre-denaturation step (5 min), followed by 35 cycles of: denaturation at 95 °C (1 min), annealing at 60 °C (1 min) and extension at 72 °C (1 min). Following the last PCR cycle, additional extension at 72 °C (10 min) was performed to ensure complete elongation of any remaining single-stranded DNA. PCR reactions were performed in a total volume of 20 uL comprised of ~1 uL of genomic

DNA (~100 ng), 1 uL of each primer (20 nM), and 0.5 uL of dNTPs (10 mM). Taq polymerase, 10X buffer and MgCl<sub>2</sub> was provided using the HotStar Taq DNA polymerase kit (Qiagen, Valencia, CA). The amplicons were resolved by gel electrophoresis on 2% agarose gels, which were run with a 2 kb molecular weight standard (Lo DNA Marker, Bionexus, Oakland CA). Images were captured using a gel imaging software system (Quantity One 1-D Analysis Software, Bio-Rad, Hercules, CA).

**Protocol - cell culture and nuclei preparation.** Male bovine kidney (MDBK, ATCC: CCL-22, Bethesda, MD) and female bovine fibroblast (Minitube, Verona, WI) cell lines were maintained in DMEM with GlutaMax (Gibco, 10569-010) and 10% fetal bovine serum (Invitrogen). The cell lines were cultured in separate 25 mL flasks at 38.5 °C in a 5% CO<sub>2</sub> atmosphere for 24-72 h to achieve confluent growth. Following this, the medium was treated with colcemid for 2h and then replaced with 0.25% trypsin-EDTA in DMEM. The cells were cultured for 20 min as stated above to detach adherent cells. The loosened cells were aspirated and transferred to 15 mL centrifuge tubes and centrifuged at 600x g for 4 min to pellet the cells. The supernatant was aspirated off, replaced with 75 mM KCl (hypotonic buffer), and the cells incubated for 20 min at 37 °C. The cell suspension was centrifuged and the supernatant aspirated off. The pellet – containing somatic nuclei – was subsequently resuspended in methanol and glacial acetic acid (3:1, v/v) and stored at -20 °C until use.

**Protocol - fluorescence in situ hybridization.** An aliquot (3-5 uL) was taken from the abovementioned somatic nuclei suspension and dropped onto a plastic slide (Sex-Y™, Minitube, Verona, WI). The slide was briefly placed in an oven to fix nuclei and evaporate solvents (2 min,

60 °C) and subsequently cooled to room temperature. An aliquot (~250 uL) of the labeling buffer [~15 ng of a Cy3-labeled Invader probe in 500 uL TE buffer (10 mM Tris and 1 mM EDTA; pH 8.0)] was placed on top of the fixed nuclei. The slide was placed in a plastic culture dish, covered with a lid and moved to a 38.5 °C incubator for ~3h. Following incubation, the slide was rinsed 3 min in warm TE buffer (38.5 °C) and left to dry at room temperature. An aliquot (~3 uL) of Gold SlowFade plus DAPI (Invitrogen) was placed directly on the slide and a round coverslip was mounted for fluorescence imaging. A Zeiss AxioSkop 40 fluorescent microscope (50 W, HBO mercury lamp), equipped with Cy3 and DAPI filter sets, was used to visualize the nuclei at 400× magnification. Images of fluorescently labeled nuclei were captured using a Zeiss AxioCam MRc5 camera and processed with AxioVision (version 4.8) software. Excellent slide-to-slide reproducibility was observed using this protocol within a given batch of nuclei preparations.

Control experiments involving DNase/RNase/proteinase pre-treated MDBK nuclei included the following steps prior to incubation with Invader probes. DNase pre-treatment: approximately 1 µL DNase I (Sigma-Aldrich D7291) was diluted in 1X reaction buffer (20 mM Tris-HCl, 2 mM MgCl<sub>2</sub>, pH 8.3) and the solution was incubated with fixed nuclei for 20 min at 37 °C, followed by rinsing with TE buffer. RNase pre-treatment: approximately 1 µL RNase A (Sigma-Aldrich R4642) was diluted in 100 µL of 10 mM Tris-HCl (pH 6.5), and the solution incubated with fixed nuclei for 45 min at 37 °C, followed by rinsing with TE buffer. Proteinase pre-treatment: approximately 1 µL of proteinase K (Sigma-Aldrich P6556) was diluted in 200 µL of 10 mM Tris-HCl (pH 7.5) and the solution incubated with fixed nuclei for 1h at 37 °C, followed by rinsing with TE buffer.

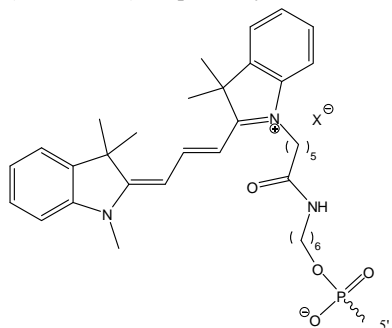
**Definition - interstrand zipper arrangement.** The following nomenclature describes the relative arrangement between two monomers positioned on opposing strands in a duplex. The number  $n$  describes the distance measured in number of base pairs and has a positive value if a monomer is shifted toward the 5'-side of its own strand relative to a second reference monomer on the other strand. Conversely,  $n$  has a negative value if a monomer is shifted toward the 3'-side of its own strand relative to a second reference monomer on the other strand.



**Table S1.** MALDI-MS of ONs modified with 2'-*O*-(pyren-1-yl)methyl-RNA monomers.<sup>a</sup>

ON	Sequence	Observed <i>m/z</i> [M+H] <sup>+</sup>	Calculated <i>m/z</i> [M+H] <sup>+</sup>
X1*	5'-GG <u>X</u> ATA TAT AGG C	4228	4228
X2*	3'-CCA <u>X</u> AT ATA TCC G	4108	4108
X3	5'-GGT A <u>X</u> A TAT AGG C	4228	4228
X4	3'-CCA TA <u>X</u> ATA TCC G	4108	4108
X5*	5'-GGT ATA <u>X</u> AT AGG C	4228	4228
X6*	3'-CCA TAT A <u>X</u> A TCC G	4108	4108
X7*	5'-GGT ATA TA <u>X</u> AGG C	4228	4228
X8*	3'-CCA TAT ATA <u>X</u> CC G	4108	4108
X9*	5'-GG <u>X</u> A <u>X</u> A TAT AGG C	4444	4444
X10*	3'-CCA <u>X</u> A <u>X</u> ATA TCC G	4324	4324
X11	5'-GG <u>X</u> ATA <u>X</u> AT AGG C	4444	4444
X12	3'-CCA <u>X</u> AT A <u>X</u> A TCC G	4324	4324
X13	5'-GG <u>X</u> ATA TA <u>X</u> AGG C	4444	4444
X14	3'-CCA <u>X</u> AT ATA <u>X</u> CC G	4324	4324
X15	5'-GGT A <u>X</u> A <u>X</u> AT AGG C	4444	4444
X16	3'-CCA TA <u>X</u> A <u>X</u> A TCC G	4324	4324
X17	5'-GGT ATA <u>X</u> A <u>X</u> AGG C	4444	4444
X18	3'-CCA TAT A <u>X</u> A <u>X</u> CC G	4324	4324
X19	5'-GG <u>X</u> A <u>X</u> A <u>X</u> A <u>X</u> AGG C	4876	4876
X20	3'-CCA <u>X</u> A <u>X</u> A <u>X</u> A <u>X</u> CC G	4757	4756
A1	3'-CCA <u>A</u> TAT ATA TCC G	4122	4122
A2	3'-CCA T <u>A</u> T ATA TCC G	4122	4122
A3	3'-CCA TAT <u>A</u> TA TCC G	4122	4122
A4	3'-CCA TAT ATA <u>A</u> TCC G	4122	4122
A5	3'-CCA T <u>A</u> T <u>A</u> TA TCC G	4352	4352
A6	3'-CCA <u>A</u> TAT <u>A</u> TA TCC G	4352	4352
A7	3'-CCA <u>A</u> TAT ATA <u>A</u> TCC G	4351	4352
A8	3'-CCA T <u>A</u> T <u>A</u> TA TCC G	4352	4352
A9	3'-CCA TAT <u>A</u> <u>A</u> TCC G	4351	4352
A10	3'-CCA <u>A</u> T <u>A</u> T <u>A</u> <u>A</u> TCC G	4813	4813
INV1-u	5'-[Cy3]-AGCCC <u>U</u> G <u>U</u> GCCCTG	5265	5265
INV1-l	3'-TCGGGAC <u>A</u> C <u>G</u> GGAC-[Cy3]	5391	5391
INV2-u	5'-[Cy3]-CC <u>U</u> G <u>U</u> GCCCTG	4334	4334
INV2-l	3'-GGAC <u>A</u> C <u>G</u> GGAC-[Cy3]	4469	4469
INV3-u	5'-[Cy3]-CC <u>U</u> GTGCC <u>C</u> TG	4348	4348
INV3-l	3'-GGAC <u>A</u> C <u>G</u> GG <u>A</u> C-[Cy3]	4469	4469
INV4-u	5'-[Cy3]- <u>A</u> GCCC <u>U</u> GTGCC <u>C</u> TG	5509	5509
INV4-l	3'-TCGGGAC <u>A</u> C <u>G</u> GG <u>A</u> C-[Cy3]	5621	5621

<sup>a</sup> **A**, **C** and **U** denote 2'-*O*-(pyren-1-yl)methyladenosine,<sup>S6</sup> 2'-*O*-(pyren-1-yl)methylcytidine<sup>S6</sup> and 2'-*O*-(pyren-1-yl)methyluridine (monomer **X**), respectively. Structure of Cy3 label shown below.



\* previously published in reference S4

**Table S2.** MALDI-MS of ONs modified with 2'-*N*-(pyren-1-ylmethyl)-2'-*N*-methylamino-uridine monomers.

ON	Sequence	Observed $m/z$ [M+H] <sup>+</sup>	Calculated $m/z$ [M+H] <sup>+</sup>
Y01	5'-GGY ATA TAT AGG C	4243	4242
Y02	3'-CCA YAT ATA TCC G	4123	4122
Y03	5'-GGT AYA TAT AGG C	4240	4242
Y04	3'-CCA TAY ATA TCC G	4121	4122
Y05	5'-GGT ATA YAT AGG C	4242	4242
Y06	3'-CCA TAT AYA TCC G	4122	4122
Y07	5'-GGT ATA TAY AGG C	4241	4242
Y08	3'-CCA TAT ATA YCC G	4121	4122
Y09	5'-GGY AYA TAT AGG C	4472	4471
Y10	3'-CCA YAY ATA TCC G	4352	4351
Y11	5'-GGY ATA YAT AGG C	4471	4471
Y12	3'-CCA YAT AYA TCC G	4351	4351
Y13	5'-GGY ATA TAY AGG C	4471	4471
Y14	3'-CCA YAT ATA YCC G	4351	4351
Y15	5'-GGT AYA YAT AGG C	4472	4471
Y16	3'-CCA TAY AYA TCC G	4351	4351
Y17	5'-GGT ATA YAY AGG C	4471	4471
Y18	3'-CCA TAT AYA YCC G	4351	4351
Y19	5'-GGY AYA YAY AGG C	4930	4929
Y20	3'-CCA YAY AYA YCC G	4811	4809

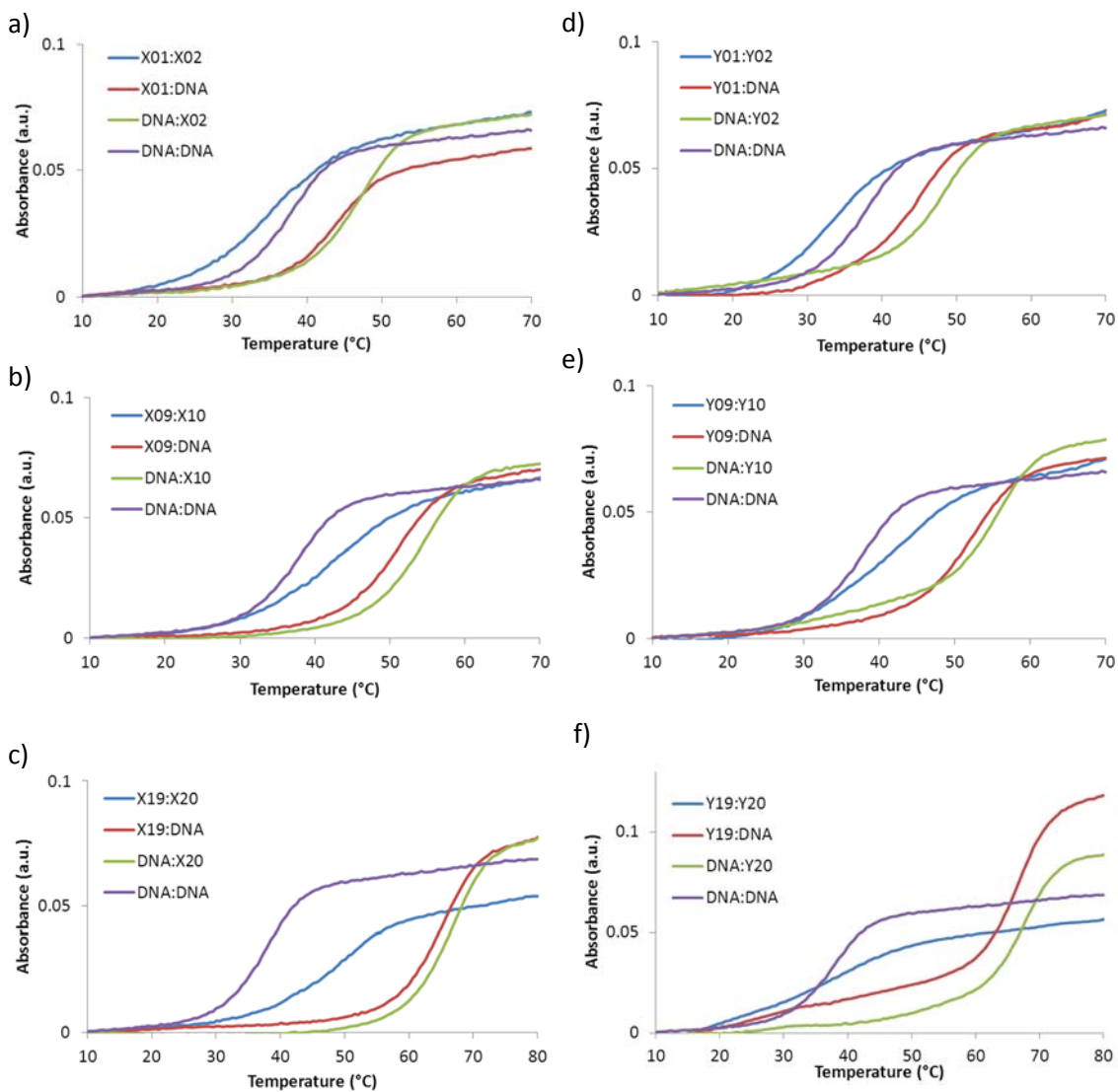


**Figure S1.** Representative thermal denaturation curves of Invader probes, corresponding duplexes between individual probe strands and cDNA, and unmodified reference duplex. For experimental conditions, see Table 1.

**Table S3.** Thermal denaturation temperatures ( $T_m$ 's) and thermal advantage ( $TA$ ) of DNA duplexes modified with 2'-*O*-(pyren-1-yl)methyluridine monomers.<sup>a</sup>

ON	Sequence	Zipper	$T_m$ [ $\Delta T_m$ ] (°C)		$TA$ (°C)
			Probe duplex	5'-ON:cDNA 3'-ON:cDNA	
X1	5'-GG <u>X</u> ATATATAGGC	+7	53.0	44.5 [+7.0]	+0.5
X8	3'-CCATATATA <u>X</u> CCG		[+15.5]	46.5 [+9.0]	
X1	5'-GG <u>X</u> ATATATAGGC	+5	55.5	44.5 [+7.0]	-1.0
X6	3'-CCATATA <u>X</u> ATCCG		[+18.0]	47.5 [+10.0]	
X3	5'-GGT <u>X</u> ATATAGGC	+5	56.0	47.5 [+10.0]	+0.5
X8	3'-CCATATATA <u>X</u> CCG		[+18.5]	46.5 [+9.0]	
X1	5'-GG <u>X</u> ATATATAGGC	+3	54.0	44.5 [+7.0]	+1.5
X4	3'-CCATA <u>X</u> ATATCCG		[+16.5]	48.5 [+11.0]	
X3	5'-GGT <u>X</u> ATATAGGC	+3	57.0	47.5 [+10.0]	+0.5
X6	3'-CCATATA <u>X</u> ATCCG		[+19.5]	47.5 [+10.0]	
X5	5'-GGTATA <u>X</u> ATAGGC	+3	56.0	48.5 [+11.0]	+1.5
X8	3'-CCATATATA <u>X</u> CCG		[+18.5]	46.5 [+9.0]	
X3	5'-GGT <u>X</u> ATATAGGC	-1	53.0	47.5 [+10.0]	+4.5
X2	3'-CC <u>X</u> ATATATCCG		[+15.5]	47.5 [+10.0]	
X5	5'-GGTATA <u>X</u> ATAGGC	-1	55.0	48.5 [+11.0]	+4.5
X4	3'-CCATA <u>X</u> ATATCCG		[+17.5]	48.5 [+11.0]	
X7	5'-GGTATATA <u>X</u> AGGC	-1	54.0	47.5 [+10.0]	+3.5
X6	3'-CCATATA <u>X</u> ATCCG		[+16.5]	47.5 [+10.0]	
X5	5'-GGTATA <u>X</u> ATAGGC	-3	57.0	48.5 [+11.0]	+1.5
X2	3'-CC <u>X</u> ATATATCCG		[+19.5]	47.5 [+10.0]	
X7	5'-GGTATATA <u>X</u> AGGC	-3	57.0	47.5 [+10.0]	+1.5
X4	3'-CCATA <u>X</u> ATATCCG		[+19.5]	48.5 [+11.0]	
X7	5'-GGTATATA <u>X</u> AGGC	-5	57.0	47.5 [+10.0]	+0.5
X2	3'-CC <u>X</u> ATATATCCG		[+19.5]	47.5 [+10.0]	

<sup>a</sup>  $\Delta T_m$  = change in  $T_m$  relative to corresponding unmodified DNA duplex ( $T_m = 37.5$  °C). For experimental conditions and definition of  $TA$ , see Table 1.

**Table S4.** Thermal denaturation temperatures ( $T_m$ 's) and thermal advantage ( $TA$ ) of DNA duplexes modified with 2'-*N*-(pyren-1-ylmethyl)-2'-*N*-methylaminouridine monomers.<sup>a</sup>

ON	Sequence	Zipper	$T_m$ [ $\Delta T_m$ ] (°C)		$TA$ (°C)
			Probe duplex	5'-ON:cDNA 3'-ON:cDNA	
Y1	5'-GGY <u>Y</u> ATATATAGGC	+7	55.5	45.5 [+8.0]	+0.5
Y8	3'-CCATATATA <u>Y</u> CCG		[+18.0]	48.0 [+10.5]	
Y1	5'-GGY <u>Y</u> ATATATAGGC	+5	56.0	45.5 [+8.0]	+1.0
Y6	3'-CCATATA <u>Y</u> ATCCG		[+18.5]	49.0 [+11.5]	
Y3	5'-GGTAY <u>Y</u> ATATAGGC	+5	58.0	48.5 [+11.0]	+1.0
Y8	3'-CCATATATA <u>Y</u> CCG		[+20.5]	48.0 [+10.5]	
Y1	5'-GGY <u>Y</u> ATATATAGGC	+3	56.0	45.5 [+8.0]	+3.0
Y4	3'-CCATA <u>Y</u> ATATCCG		[+18.5]	51.0 [+13.5]	
Y3	5'-GGTAY <u>Y</u> ATATAGGC	+3	57.5	48.5 [+11.0]	+2.5
Y6	3'-CCATATA <u>Y</u> ATCCG		[+20.0]	49.0 [+11.5]	
Y5	5'-GGTATA <u>Y</u> ATAGGC	+3	57.0	49.5 [+12.0]	+3.0
Y8	3'-CCATATATA <u>Y</u> CCG		[+19.5]	48.0 [+10.5]	
Y3	5'-GGTAY <u>Y</u> ATATAGGC	-1	54.5	48.5 [+11.0]	+4.0
Y2	3'-CCA <u>Y</u> ATATATCCG		[+17.0]	47.5 [+10.0]	
Y5	5'-GGTATA <u>Y</u> ATAGGC	-1	57.0	49.5 [+12.0]	+6.0
Y4	3'-CCATA <u>Y</u> ATATCCG		[+19.5]	51.0 [+13.5]	
Y7	5'-GGTATATA <u>Y</u> AGGC	-1	54.5	48.0 [+10.5]	+4.5
Y6	3'-CCATATA <u>Y</u> ATCCG		[+17.0]	49.0 [+11.5]	
Y5	5'-GGTATA <u>Y</u> ATAGGC	-3	58.5	49.5 [+12.0]	+1.0
Y2	3'-CCA <u>Y</u> ATATATCCG		[+21.0]	47.5 [+10.0]	
Y7	5'-GGTATATA <u>Y</u> AGGC	-3	59.5*	48.0 [+10.5]	+2.0
Y4	3'-CCATA <u>Y</u> ATATCCG		[+22.0]	51.0 [+13.5]	
Y7	5'-GGTATATA <u>Y</u> AGGC	-5	58.5	48.0 [+10.5]	-0.5
Y2	3'-CCA <u>Y</u> ATATATCCG		[+21.0]	47.5 [+10.0]	

<sup>a</sup>  $\Delta T_m$  = change in  $T_m$  relative to corresponding unmodified DNA duplex ( $T_m = 37.5$  °C). For experimental conditions and definition of  $TA$ , see Table 1.

\* Two transitions were observed ( $T_m = \sim 25$  °C and 59.5 °C) suggesting a complicated melting transition.

**Table S5.** Thermal denaturation temperatures ( $T_m$ 's) and thermal advantage ( $TA$ ) of DNA duplexes modified with 0-zippers of 2'-*O*-(pyren-1-yl)methyl-RNA monomers.<sup>a</sup>

ON	Sequence	Zipper	$T_m$ [ $\Delta T_m$ ] (°C)		$TA$ (°C)
			Probe duplex	5'-ON:cDNA 3'-ON:cDNA	
X1	5'-GGXATATATAGGC	0	38.0	44.5 [+7.0]	+3.0
A1	3'-CCATATATATCCG		[+0.5]	34.0 [-3.5]	
X3	5'-GGTAXATATAGGC	0	40.0	47.5 [+10.0]	+1.0
A2	3'-CCATATATATCCG		[+2.5]	31.0 [-6.5]	
X5	5'-GGTATAXATAGGC	0	40.0	48.5 [+11.0]	+2.0
A3	3'-CCATATATATCCG		[+2.5]	31.0 [-6.5]	
X7	5'-GGTATATAXAGGC	0	40.0	47.5 [+10.0]	+1.0
A4	3'-CCATATATATCCG		[+2.5]	31.0 [-6.5]	
X9	5'-GGXAXATATAGGC	0	41.0	51.5 [+14.0]	±0.0
A5	3'-CCATATATATCCG		[+3.5]	27.0 [-10.5]	
X11	5'-GGXATAXATAGGC	0	41.0	53.5 [+16.0]	+1.0
A6	3'-CCATATATATCCG		[+3.5]	26.0 [-11.5]	
X13	5'-GGXATATAXAGGC	0	42.0	52.5 [+15.0]	-1.0
A7	3'-CCATATATATCCG		[+4.5]	26.0 [-11.5]	
X15	5'-GGTAXAXATAGGC	0	42.0	55.5 [+18.0]	+2.0
A8	3'-CCATATATATCCG		[+4.5]	26.0 [-11.5]	
X17	5'-GGTATAXAXAGGC	0	42.0	54.5 [+17.0]	+1.0
A9	3'-CCATATATATCCG		[+4.5]	26.0 [-11.5]	
X19	5'-GGXAXAXAXAGGC	0	44.0	65.5 [+28.0]	+27.0
A10	3'-CCATATATATCCG		[+6.5]	43.0 [+5.5]	

<sup>a</sup>  $\Delta T_m$  = change in  $T_m$  relative to corresponding unmodified DA duplex ( $T_m = 37.5$  °C). For experimental conditions and definition of  $TA$ , see Table 1. **A** = 2'-*O*-(pyren-1-yl)methyladenosine monomer.<sup>S6</sup>

**Table S6.** Change in Gibbs free energy ( $\Delta G$ ) at 293K upon formation of X-modified DNA duplexes and change in reaction free energy upon hypothetical Invader-mediated recognition of isosequential dsDNA targets ( $\Delta G_{rec}^{293}$ ).<sup>a</sup>

ON	Sequence	$\Delta G^{293} [\Delta \Delta G^{293}]$ (kJ/mol)			$\Delta G_{rec}^{293}$ (kJ/mol)
		5'-Inv:cDNA	3'-Inv:cDNA	Invader	
<b>X1</b>	5'-GGXATATATAGGC	-64 [-7]	-67 [-10]	-47 [+10]	-27
<b>X2</b>	3'-CCA <del>X</del> ATATATCCG				
<b>X3</b>	5'-GGTAXATATAGGC	-70 [-13]	-69 [-12]	-50 [+7]	-32
<b>X4</b>	3'-CCATA <del>X</del> ATATCCG				
<b>X5</b>	5'-GGTATA <del>X</del> ATAGGC	-70 [-13]	-71 [-14]	-52 [+5]	-32
<b>X6</b>	3'-CCATATA <del>X</del> ATCCG				
<b>X7</b>	5'-GGTATATA <del>X</del> AGGC	-68 [-11]	-66 [-9]	-46 [+11]	-31
<b>X8</b>	3'-CCATATATA <del>X</del> CCG				
<b>X9</b>	5'-GG <del>X</del> A <del>X</del> ATATAGGC	-71 [-14]	-77 [-20]	-51 [+6]	-40
<b>X10</b>	3'-CCA <del>X</del> A <del>X</del> ATATCCG				
<b>X11</b>	5'-GGXATA <del>X</del> ATAGGC	-78 [-21]	-83 [-26]	-58 [-1]	-46
<b>X12</b>	3'-CCA <del>X</del> ATA <del>X</del> ATCCG				
<b>X13</b>	5'-GGXATATA <del>X</del> AGGC	-75 [-18]	-79 [-22]	-59 [-2]	-38
<b>X14</b>	3'-CCA <del>X</del> ATATA <del>X</del> CCG				
<b>X15</b>	5'-GGTAXA <del>X</del> ATAGGC	-81 [-24]	-78 [-21]	-57 [ $\pm$ 0]	-45
<b>X16</b>	3'-CCATA <del>X</del> A <del>X</del> ATCCG				
<b>X17</b>	5'-GGTATA <del>X</del> A <del>X</del> AGGC	-77 [-20]	-80 [-23]	-54 [+3]	-46
<b>X18</b>	3'-CCATATA <del>X</del> A <del>X</del> CCG				
<b>X19</b>	5'-GG <del>X</del> A <del>X</del> A <del>X</del> A <del>X</del> AGGC	-91 [-34]	-92 [-35]	-55 [+2]	-71
<b>X20</b>	3'-CCA <del>X</del> A <del>X</del> A <del>X</del> A <del>X</del> CCG				

<sup>a</sup>  $\Delta \Delta G^{293}$  is measured relative to the corresponding unmodified DNA duplex ( $\Delta G^{293} = -57$  kJ/mol).  $\Delta G_{rec}^{293} = \Delta G^{293}$  (5'-Inv:cDNA)

+  $\Delta G^{293}$  (3'-Inv:cDNA) -  $\Delta G^{293}$  (Invader) -  $\Delta G^{293}$  (dsDNA).

**Table S7.** Change in Gibbs free energy ( $\Delta G$ ) at 293K upon formation of Y-modified DNA duplexes and change in reaction free energy upon hypothetical Invader-mediated recognition of isosequential dsDNA targets ( $\Delta G_{rec}^{293}$ ).<sup>a</sup>

ON	Sequence	$\Delta G^{293}[\Delta\Delta G^{293}]$ (kJ/mol)			$\Delta G_{rec}^{293}$ (kJ/mol)
		5'-Inv:cDNA	3'-Inv:cDNA	Invader	
<b>Y1</b>	5'-GGYATATATAGGC				
<b>Y2</b>	3'-CCAYATATATCCG	-63 [-6]	-79 [-22]	-50 [+7]	-35
<b>Y3</b>	5'-GGTAYATATAGGC				
<b>Y4</b>	3'-CCATAYATATCCG	-75 [-18]	-82 [-25]	-62 [-5]	-38
<b>Y5</b>	5'-GGTATAYATAGGC				
<b>Y6</b>	3'-CCATATAYATCCG	-76 [-19]	-79 [-22]	-59 [-2]	-39
<b>Y7</b>	5'-GGTATATAYAGGC				
<b>Y8</b>	3'-CCATATATAYCCG	-74 [-17]	-78 [-21]	-54 [+3]	-41
<b>Y9</b>	5'-GGYAYATATAGGC				
<b>Y10</b>	3'-CCAYAYATATCCG	-80 [-23]	-94 [-37]	-54 [+3]	-63
<b>Y11</b>	5'-GGYATAYATAGGC				
<b>Y12</b>	3'-CCAYATAYATCCG	-86 [-29]	-92 [-35]	-63 [-6]	-58
<b>Y13</b>	5'-GGYATATAYAGGC				
<b>Y14</b>	3'-CCAYATATAYCCG	-84 [-27]	-100 [-43]	-58 [-1]	-69
<b>Y15</b>	5'-GGTAYAYATAGGC				
<b>Y16</b>	3'-CCATAYAYATCCG	-85 [-28]	-93 [-36]	-54 [+3]	-67
<b>Y17</b>	5'-GGTATAYAYAGGC				
<b>Y18</b>	3'-CCATATAYAYCCG	-83 [-26]	-84 [-27]	-61 [-4]	-49
<b>Y19</b>	5'-GGYAYAYAYAGGC				
<b>Y20</b>	3'-CCAYAYAYAYCCG	-109 [-52]	-101 [-44]	-58 [-1]	-95

<sup>a</sup>  $\Delta\Delta G^{293}$  is measured relative to the corresponding unmodified DNA duplex ( $\Delta G^{293} = -57$  kJ/mol).  $\Delta G_{rec}^{293} = \Delta G^{293}$  (5'-Inv:cDNA)

+  $\Delta G^{293}$  (3'-Inv:cDNA) -  $\Delta G^{293}$  (Invader) -  $\Delta G^{293}$  (dsDNA).



**Table S8.** Change in enthalpy ( $\Delta H$ ) upon formation of X-modified duplexes and change in reaction enthalpy upon hypothetical Invader-mediated recognition of isosequential dsDNA targets ( $\Delta H_{\text{rec}}$ ).<sup>a</sup>

ON	Sequence	$\Delta H$ [ $\Delta\Delta H$ ] (kJ/mol)			$\Delta H_{\text{rec}}$ (kJ/mol)
		5'-Inv:cDNA	3'-Inv:cDNA	Invader	
<b>X1</b>	5'-GG <u>X</u> ATATATAGGC	-410 [-28]	-410 [-28]	-266 [+116]	-172
<b>X2</b>	3'-CC <u>A</u> XATATATCCG				
<b>X3</b>	5'-GGT <u>A</u> XATATAGGC	-430 [-48]	-414 [-32]	-301 [+81]	-161
<b>X4</b>	3'-CCAT <u>A</u> XATATCCG				
<b>X5</b>	5'-GGTAT <u>A</u> XATAGGC	-434 [-52]	-451 [-69]	-328 [+54]	-175
<b>X6</b>	3'-CCATAT <u>A</u> XATCCG				
<b>X7</b>	5'-GGTATAT <u>A</u> XAGGC	-418 [-36]	-402 [-20]	-257 [+125]	-181
<b>X8</b>	3'-CCATATAT <u>A</u> XCCG				
<b>X9</b>	5'-GG <u>X</u> <u>A</u> XATATAGGC	-402 [-20]	-416 [-34]	-257 [+125]	-179
<b>X10</b>	3'-CC <u>A</u> <u>X</u> <u>A</u> XATATCCG				
<b>X11</b>	5'-GG <u>X</u> AT <u>A</u> XATAGGC	-438 [-56]	-454 [-72]	-286 [+96]	-224
<b>X12</b>	3'-CC <u>A</u> <u>X</u> AT <u>A</u> XATCCG				
<b>X13</b>	5'-GG <u>X</u> ATAT <u>A</u> XAGGC	-423 [-41]	-437 [-55]	-296 [+86]	-182
<b>X14</b>	3'-CC <u>A</u> <u>X</u> ATAT <u>A</u> XCCG				
<b>X15</b>	5'-GGT <u>A</u> <u>X</u> <u>A</u> XATAGGC	-457 [-75]	-423 [-41]	-317 [+65]	-181
<b>X16</b>	3'-CCAT <u>A</u> <u>X</u> <u>A</u> XATCCG				
<b>X17</b>	5'-GGTAT <u>A</u> <u>X</u> <u>A</u> XAGGC	-427 [-45]	-424 [-42]	-260 [+122]	-209
<b>X18</b>	3'-CCATAT <u>A</u> <u>X</u> <u>A</u> XCCG				
<b>X19</b>	5'-GG <u>X</u> <u>A</u> <u>X</u> <u>A</u> <u>X</u> AGGC	-434 [-52]	-424 [-42]	-256 [+126]	-220
<b>X20</b>	3'-CC <u>A</u> <u>X</u> <u>A</u> <u>X</u> <u>A</u> XCCG				

<sup>a</sup>  $\Delta\Delta H$  is measured relative to the corresponding unmodified DNA duplex ( $\Delta H = -382$  kJ/mol).  $\Delta H_{\text{rec}} = \Delta H(5'\text{-Inv:cDNA}) + \Delta H$

(3'-Inv:cDNA) -  $\Delta H$  (Invader) -  $\Delta H$  (dsDNA).

**Table S9.** Change in enthalpy ( $\Delta H$ ) upon formation of Y-modified duplexes and change in reaction enthalpy upon hypothetical Invader-mediated recognition of isosequential dsDNA targets ( $\Delta H_{\text{rec}}$ ).<sup>a</sup>

ON	Sequence	$\Delta H$ [ $\Delta\Delta H$ ] (kJ/mol)			$\Delta H_{\text{rec}}$ (kJ/mol)
		5'-Inv:cDNA	3'-Inv:cDNA	Invader	
Y1	5'-GGYATATATAGGC	-352 [+30]	-480 [-98]	-295 [+87]	-155
Y2	3'-CCAYATATATCCG				
Y3	5'-GGTAYATATAGGC	-429 [-47]	-463 [-81]	-375 [+7]	-135
Y4	3'-CCATAYATATCCG				
Y5	5'-GGTATAYATAGGC	-441 [-59]	-466 [-84]	-382 [ $\pm 0$ ]	-143
Y6	3'-CCATATAYATCCG				
Y7	5'-GGTATATAYAGGC	-429 [-47]	-470 [-88]	-287 [+95]	-230
Y8	3'-CCATATATAYCCG				
Y9	5'-GGYAYATATAGGC	-442 [-60]	-539 [-157]	-247 [+135]	-352
Y10	3'-CCAYAYATATCCG				
Y11	5'-GGYATAYATAGGC	-448 [-66]	-482 [-100]	-307 [+75]	-241
Y12	3'-CCAYATAYATCCG				
Y13	5'-GGYATATAYAGGC	-444 [-62]	-546 [-164]	-269 [+113]	-342
Y14	3'-CCAYATATAYCCG				
Y15	5'-GGTAYAYATAGGC	-447 [-65]	-519 [-137]	-305 [+77]	-279
Y16	3'-CCATAYAYATCCG				
Y17	5'-GGTATAYAYAGGC	-437 [-55]	-439 [-57]	-293 [+89]	-201
Y18	3'-CCATATAYAYCCG				
Y19	5'-GGYAYAYAYAGGC	-527 [-145]	-465 [-83]	-297 [+85]	-313
Y20	3'-CCAYAYAYAYCCG				

<sup>a</sup>  $\Delta\Delta H$  is measured relative to the corresponding unmodified DNA duplex ( $\Delta H = -382$  kJ/mol).  $\Delta H_{\text{rec}} = \Delta H(5'\text{-Inv:cDNA}) + \Delta H(3'\text{-Inv:cDNA}) - \Delta H(\text{Invader}) - \Delta H(\text{dsDNA})$ .

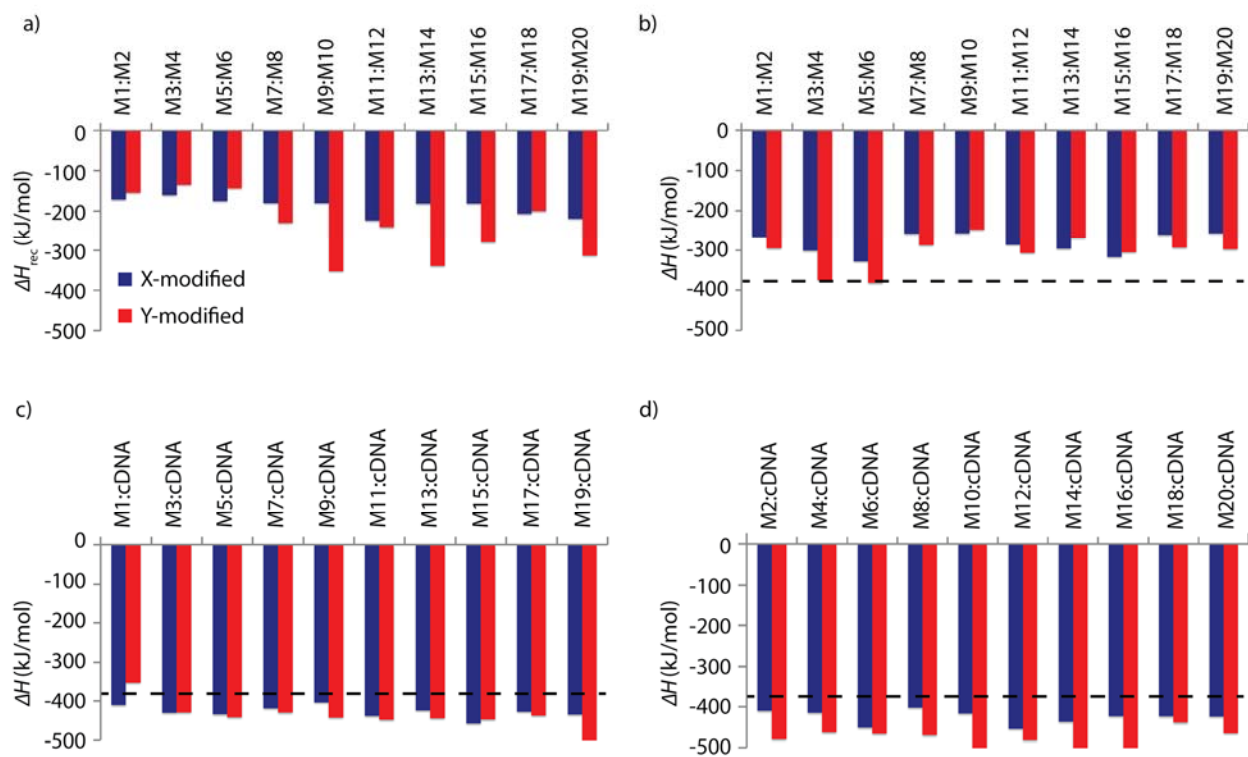


**Figure S2.** (a) Change in reaction enthalpy upon hypothetical Invader-mediated recognition of isosequential dsDNA targets ( $\Delta H_{rec}$ ), and (b-d) change in enthalpy ( $\Delta H$ ) upon formation of X- or Y-modified DNA duplexes. The  $\Delta H$  for the dsDNA reference is shown as a dotted line at -382 kJ/mol. See Table 1 for experimental conditions. See Tables S8 and S9 for tabulated data.

**Table S10.** Change in entropy at 293K ( $-T^{293}\Delta S$ ) upon formation of X-modified duplexes and change in reaction entropy upon hypothetical Invader-mediated recognition of isosequential dsDNA targets ( $-T^{293}\Delta S_{rec}$ ).<sup>a</sup>

ON	Sequence	$-T^{293}\Delta S$ [ $\Delta(T^{293}\Delta S)$ ] (kJ/mol)			$-T^{293}\Delta S_{rec}$ (kJ/mol)
		5'-Inv:cDNA	3'-Inv:cDNA	Invader	
<b>X1</b>	5'-GGXATATATAGGC	346 [+21]	342 [+17]	219 [-106]	144
<b>X2</b>	3'-CCAXATATATCCG				
<b>X3</b>	5'-GGTAXATATAGGC	358 [+33]	345 [+20]	251 [-74]	127
<b>X4</b>	3'-CCATAXATATCCG				
<b>X5</b>	5'-GGTATAXATAGGC	363 [+38]	380 [+55]	276 [-49]	142
<b>X6</b>	3'-CCATATAXATCCG				
<b>X7</b>	5'-GGTATATAXAGGC	350 [+25]	336 [+11]	211 [-114]	150
<b>X8</b>	3'-CCATATATAXCCG				
<b>X9</b>	5'-GGXAXATATAGGC	331 [+6]	339 [+14]	205 [-120]	140
<b>X10</b>	3'-CCAXAXATATCCG				
<b>X11</b>	5'-GGXATAXATAGGC	360 [+35]	371 [+46]	228 [-97]	178
<b>X12</b>	3'-CCAXATAXATCCG				
<b>X13</b>	5'-GGXATATAXAGGC	348 [+23]	357 [+32]	237 [-88]	143
<b>X14</b>	3'-CCAXATATAXCCG				
<b>X15</b>	5'-GGTAXAXATAGGC	376 [+51]	345 [+20]	260 [-65]	136
<b>X16</b>	3'-CCATAXAXATCCG				
<b>X17</b>	5'-GGTATAXAXAGGC	349 [+24]	344 [+19]	205 [-120]	163
<b>X18</b>	3'-CCATATAXAXCCG				
<b>X19</b>	5'-GGXAXAXAXAGGC	343 [+18]	332 [+7]	201 [-124]	149
<b>X20</b>	3'-CCAXAXAXAXCCG				

<sup>a</sup>  $\Delta(T^{293}\Delta S)$  is measured relative to the corresponding unmodified DNA duplex ( $-T^{293}\Delta S = 325$  kJ/mol).  $-T^{293}\Delta S_{rec} = \Delta(T^{293}\Delta S)$  (5'-

Inv:cDNA) +  $\Delta(T^{293}\Delta S)$  (3'-Inv:cDNA) -  $\Delta(T^{293}\Delta S)$  (Invader).

**Table S11.** Change in entropy at 293K ( $-T^{293}\Delta S$ ) upon formation of Y-modified duplexes and change in reaction entropy upon hypothetical Invader-mediated recognition of isosequential dsDNA targets ( $-T^{293}\Delta S_{rec}$ ).<sup>a</sup>

ON	Sequence	$-T^{293}\Delta S$ [ $\Delta(T^{293}\Delta S)$ ] (kJ/mol)			$-T^{293}\Delta S_{rec}$ (kJ/mol)
		5'-Inv:cDNA	3'-Inv:cDNA	Invader	
<b>Y1</b>	5'-GGYATATATAGGC	289 [-36]	401 [+76]	245 [-80]	120
<b>Y2</b>	3'-CCAYATATATCCG				
<b>Y3</b>	5'-GGTAYATATAGGC	354 [+29]	381 [+56]	313 [-12]	97
<b>Y4</b>	3'-CCATAYATATCCG				
<b>Y5</b>	5'-GGTATAYATAGGC	365 [+40]	387 [+62]	322 [-3]	105
<b>Y6</b>	3'-CCATATAYATCCG				
<b>Y7</b>	5'-GGTATATAYAGGC	355 [+30]	392 [+67]	233 [-92]	189
<b>Y8</b>	3'-CCATATATAYCCG				
<b>Y9</b>	5'-GGYAYATATAGGC	362 [+37]	445 [+120]	194 [-131]	288
<b>Y10</b>	3'-CCAYAYATATCCG				
<b>Y11</b>	5'-GGYATAYATAGGC	361 [+36]	389 [+64]	239 [-86]	186
<b>Y12</b>	3'-CCAYATAYATCCG				
<b>Y13</b>	5'-GGYATATAYAGGC	359 [+34]	446 [+121]	211 [-114]	269
<b>Y14</b>	3'-CCAYATATAYCCG				
<b>Y15</b>	5'-GGTAYAYATAGGC	362 [+37]	426 [+101]	250 [-75]	213
<b>Y16</b>	3'-CCATAYAYATCCG				
<b>Y17</b>	5'-GGTATAYAYAGGC	353 [+28]	355 [+30]	232 [-93]	151
<b>Y18</b>	3'-CCATATAYAYCCG				
<b>Y19</b>	5'-GGYAYAYAYAGGC	418 [+93]	364 [+39]	240 [-85]	217
<b>Y20</b>	3'-CCAYAYAYAYCCG				

<sup>a</sup>  $\Delta(T^{293}\Delta S)$  is measured relative to the corresponding unmodified DNA duplex ( $-T^{293}\Delta S = 325$  kJ/mol).  $-T^{293}\Delta S_{rec} = \Delta(T^{293}\Delta S)$  (5'-

Inv:cDNA) +  $\Delta(T^{293}\Delta S)$  (3'-Inv:cDNA) -  $\Delta(T^{293}\Delta S)$  (Invader).

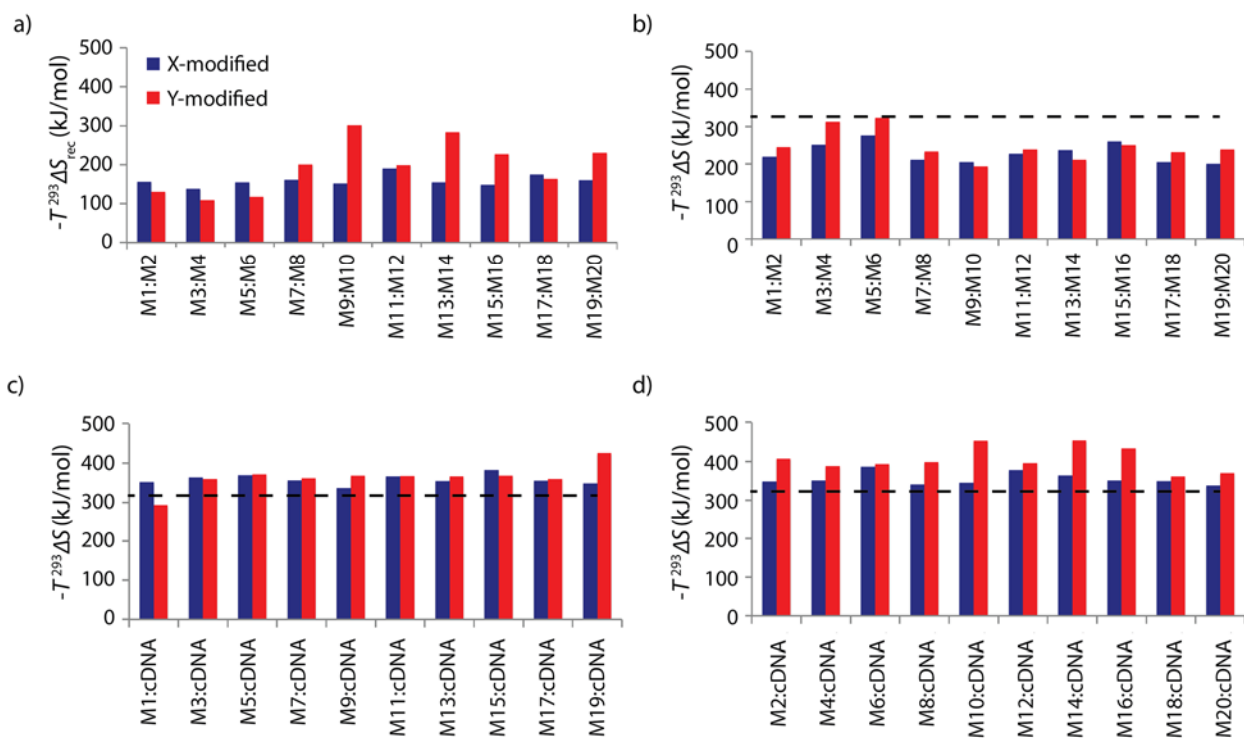
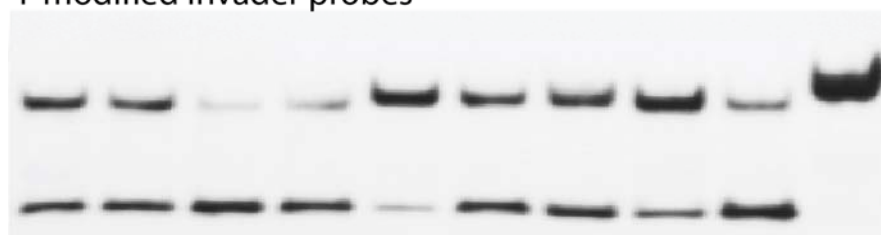


**Figure S3.** (a) Change in reaction entropy upon hypothetical Invader-mediated recognition of isosequential dsDNA targets ( $-T^{293}\Delta S_{rec}$ ), and (b-d) change in entropy ( $-T^{293}\Delta S$ ) upon formation of X- or Y-modified DNA duplexes. The  $-T^{293}\Delta S$  for the dsDNA reference is shown as a dotted line at 325 kJ/mol. See Table 1 for experimental conditions. See Tables S10 and S11 for tabulated data.

X-modified Invader probes



Y-modified Invader probes



M1:M2

M3:M4

M5:M6

M7:M8

M9:M10

M11:M12

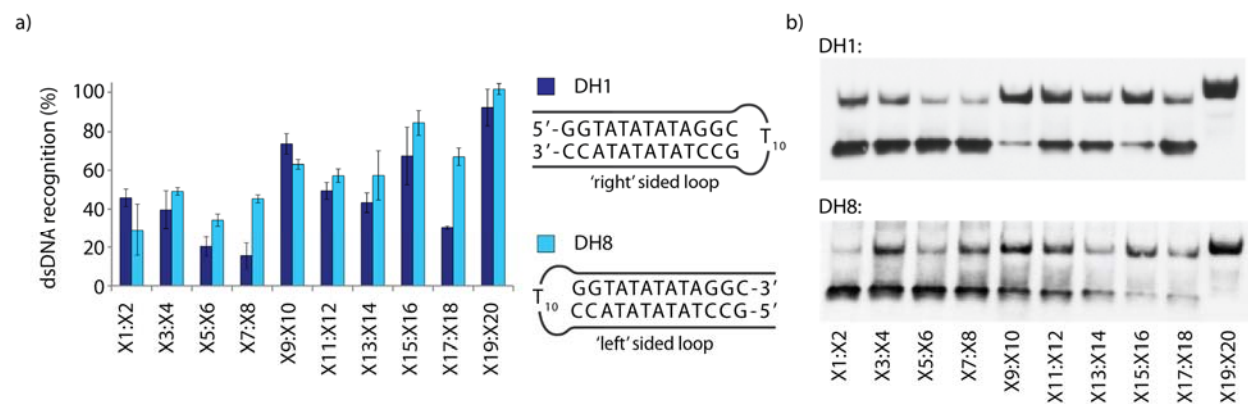
M13:M14

M15:M16

M17:M18

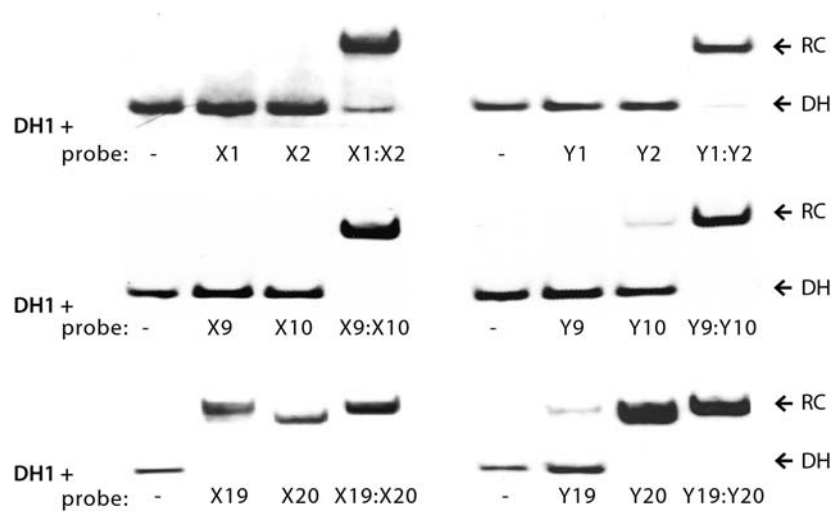
M19:M20

**Figure S4.** Representative electrophoretograms of data shown in Figure 3 of main text: dsDNA recognition by 200-fold molar excess of Invader probes modified either monomer **X** (top) or **Y** (bottom). For sequences and experimental conditions see Table 1 and Figure 3, respectively, in main text.



**Figure S5. (a)** Recognition of **DH1** or **DH8** using Invader probes **X1:X2–X19:X20** and (b) representative gel images. See Figure 3 for experimental conditions.







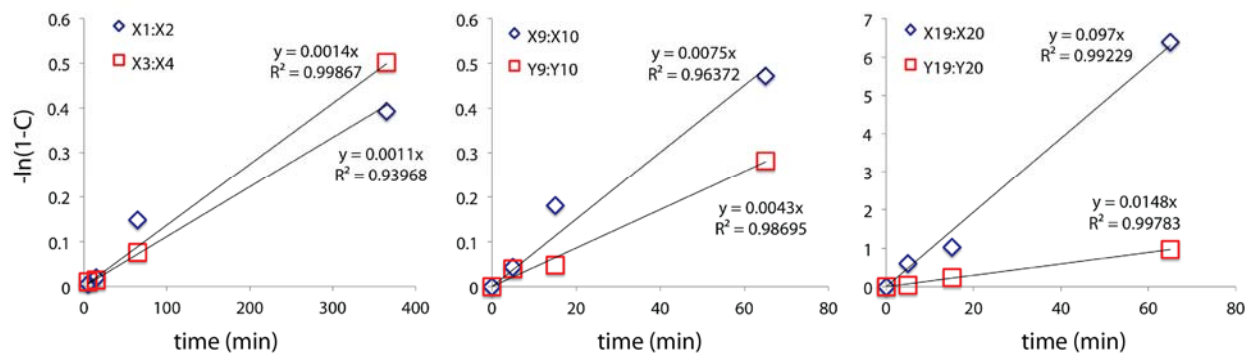






**Figure S6.** Recognition of **DH1** using individual probe strands. Single-stranded probes (and double-stranded Invader controls) were used at 1000-, 500-, or 50-fold molar excess for **M1:M2**, **M9:M10**, or **M19:M20**, respectively. For experimental conditions, see Figure 3.



**Figure S7.** Plots of  $-\ln(1-C)$  versus time, where  $C$  is the ratio of recognition complex with respect to the total hairpin concentration, used to determine pseudo-first order rate constants for initial phases of **DH1** recognition using a) **M1:M2**, b) **M9:M10**, or c) **M19:M20** at 200-fold molar excess. See Figure 3 for incubation conditions. The linearity of the plots suggests that the reaction obeys pseudo-first order kinetics.

**Table S12.** Thermal denaturation temperatures of DNA hairpin targets used in this study.

DH	Sequence	$T_m$ (°C)
1		58.5
2		60.5
3		63.5
4		63.0
5		60.0
6		62.5
7		62.5
8		59.5

<sup>a</sup> For experimental conditions, see Table 1.

**Table S13.** Change in Gibbs free energy ( $\Delta G$ ) at 310K upon formation of **X**-modified DNA duplexes and change in reaction free energy upon Invader-mediated recognition of iso-sequential dsDNA targets ( $\Delta G_{rec}^{310}$ ).<sup>a</sup>

ON	Sequence	$\Delta G^{310}[\Delta\Delta G^{310}]$ (kJ/mol)				$\Delta G_{rec}^{310}$ (kJ/mol)
		5'-Inv: cDNA	3'-Inv: cDNA	Invader	dsDNA	
INV1	5'-Cy3-AGCCCU <u>UGUG</u> CCCTG 3'-TCGGGAC <u>CAC</u> GGGAC-Cy3	-83 [-11]	-96 [-24]	-61 [+11]	-72	-46
INV2	5'-Cy3-CC <u>UGUG</u> CCCTG 3'-GGAC <u>CAC</u> GGGAC-Cy3	-60 [-7]	-71 [-18]	-48 [+5]	-53	-30
INV3	5'-Cy3-CC <u>UGTGCC</u> CTG 3'-GGAC <u>CACGGG</u> AC-Cy3	-61 [-8]	-65 [-12]	-49 [+4]	-53	-24
INV4	5'-Cy3- <u>AGCCCU</u> UGUGCCCTG 3'-T <u>CGGGAC</u> CACGGGAC-Cy3	-65 [+7]	-90 [-18]	-54 [+18]	-72	-29

<sup>a</sup>  $\Delta\Delta G^{293}$  is measured relative to the corresponding unmodified DNA duplex.  $\Delta G_{rec}^{310} = \Delta G^{310}$  (5'-

Inv:cDNA) +  $\Delta G^{310}$  (3'-Inv:cDNA) -  $\Delta G^{310}$  (Invader) -  $\Delta G^{310}$  (dsDNA).

**Table S14.** Change in enthalpy ( $\Delta H$ ) upon formation of **X**-modified duplexes and change in reaction enthalpy upon Invader-mediated recognition of iso-sequential dsDNA targets ( $\Delta H_{rec}$ ).<sup>a</sup>

ON	Sequence	$\Delta H$ [ $\Delta\Delta H$ ] (kJ/mol)				$\Delta H_{rec}$ (kJ/mol)
		5'-Inv: cDNA	3'-Inv: cDNA	Invader	dsDNA	
INV1	5'-Cy3-AGCCCUGUGCCCTG 3'-TCGGGACACGGGAC-Cy3	-476 [-7]	-539 [-70]	-342 [+127]	-469	-204
INV2	5'-Cy3-CCUGUGCCCTG 3'-GGACACGGGAC-Cy3	-333 [+21]	-391 [-37]	-210 [+144]	-354	-160
INV3	5'-Cy3-CCUGTGCCCTG 3'-GGACACGGGAC-Cy3	-350 [+4]	-350 [+4]	-213 [+141]	-354	-133
INV4	5'-Cy3-AGCCCUGUGCCCTG 3'-TCGGGACACGGGAC-Cy3	-295 [+174]	-472 [-3]	-203 [+266]	-469	-95

<sup>a</sup>  $\Delta\Delta H$  is measured relative to the corresponding unmodified DNA duplex.  $\Delta H_{rec} = \Delta H(5'-Inv:cDNA) + \Delta H(3'-Inv:cDNA) - \Delta H(Invader) - \Delta H(dsDNA)$ .

**Table S15.** Change in entropy at 310K ( $-T^{310}\Delta S$ ) upon formation of **Y**-modified duplexes and change in reaction entropy upon Invader-mediated recognition of iso-sequential dsDNA targets ( $-T^{310}\Delta S_{rec}$ ).<sup>a</sup>

ON	Sequence	$-T^{310}\Delta S$ [ $\Delta(T^{310}\Delta S)$ ] (kJ/mol)				$-T^{310}\Delta S_{rec}$ (kJ/mol)
		5'-Inv: cDNA	3'-Inv: cDNA	Invader	dsDNA	
INV1	5'-Cy3-AGCCCUGUGCCCTG 3'-TCGGGACACGGGAC-Cy3	393 [-4]	443 [+46]	281 [-116]	397	158
INV2	5'-Cy3-CCUGUGCCCTG 3'-GGACACGGGAC-Cy3	273 [-28]	320 [+19]	162 [-139]	301	130
INV3	5'-Cy3-CCUGTGCCCTG 3'-GGACACGGGAC-Cy3	289 [-12]	285 [-16]	164 [-137]	301	109
INV4	5'-Cy3-AGCCCUGUGCCCTG 3'-TCGGGACACGGGAC-Cy3	229 [-168]	382 [-15]	148 [-249]	397	66

<sup>a</sup>  $\Delta(T^{293}\Delta S)$  is measured relative to the corresponding unmodified DNA duplex.  $-T^{310}\Delta S_{rec} = \Delta(T^{310}\Delta S)(5'-Inv:cDNA) + \Delta(T^{310}\Delta S)(3'-Inv:cDNA) - \Delta(T^{310}\Delta S)(Invader)$ .

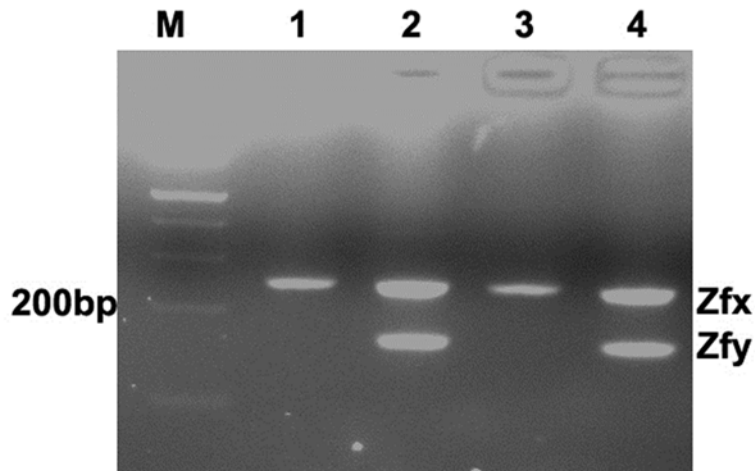


**Figure S8.** Gel electrophoretogram of gender-specific PCR amplicons. Zfx and Zfy bands represent X- and Y-chromosome specific amplicons, respectively. Lane “M” contains a molecular weight standard (Lo DNA Marker, Bionexus). PCR amplicons from female (lanes 1 and 3) and male cell lines (lanes 2 and 4). 2% agarose gels were used.

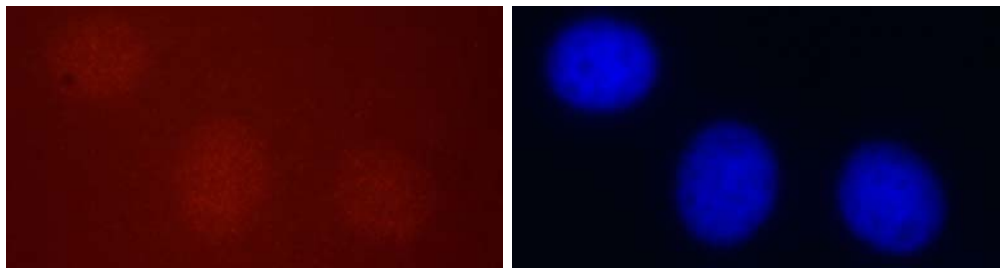


**Figure S9.** Images from FISH experiments conducted at non-denaturing conditions using nuclei from male bovine kidney cells incubated with the single-stranded Cy3-labeled PNA probe 5'-Cy3-OO-AGCCCTGTGCCCTG. Images viewed using Cy3 (left column) or DAPI (middle column) filter settings. Incubation: 3h at 38.5 °C in 10 mM Tris-Cl, pH 8.0 and 1 mM EDTA. Cells were visualized at 400x magnification using a Zeiss AxioSkop 40 fluorescent microscope and images captured using a Zeiss AxioCam MRc5 camera. "O" denotes a 9-atom ethylene glycol linker (i.e., "O-linker").

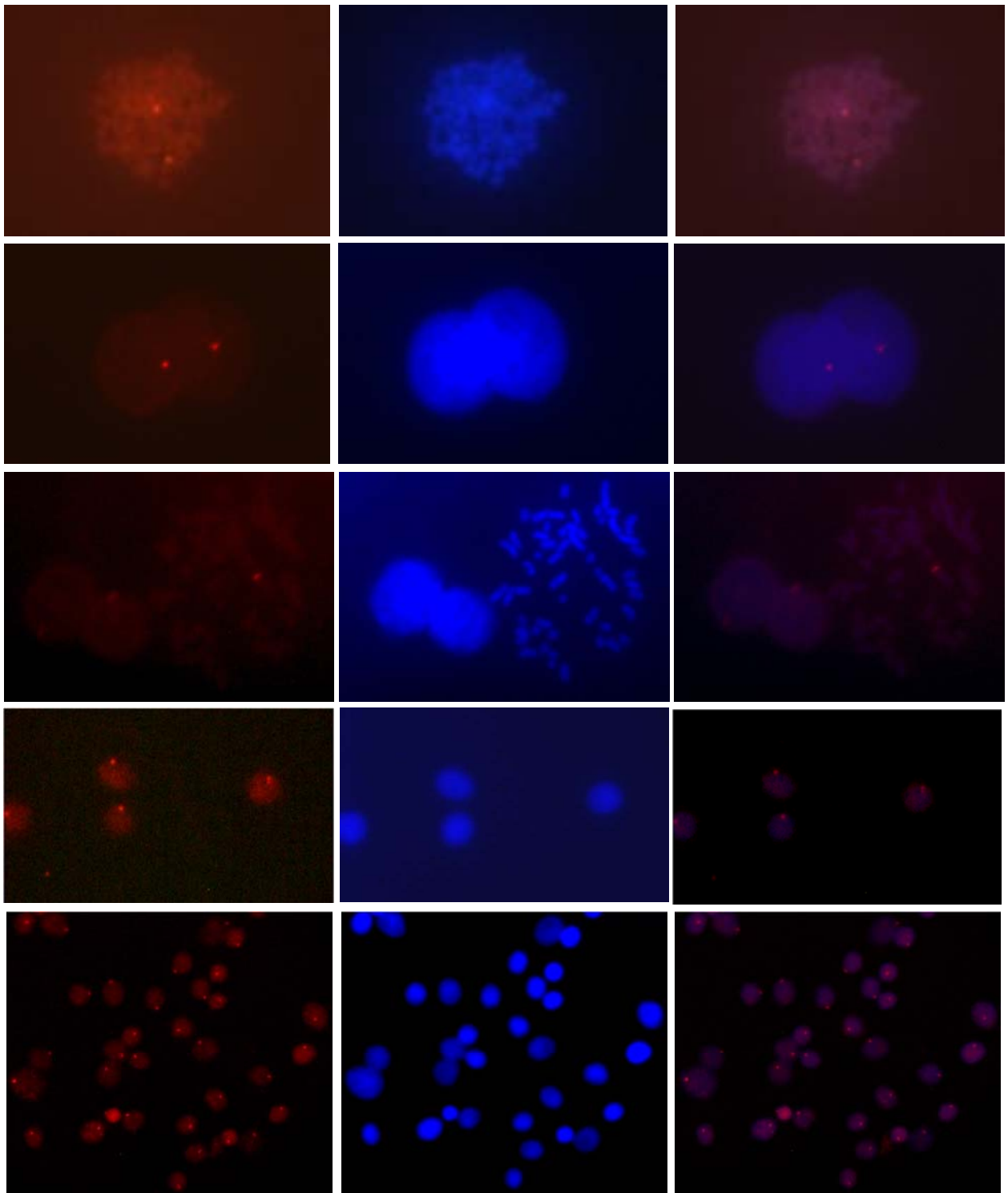


**Figure S10.** Additional images from FISH experiments using nuclei from male bovine kidney cells incubated with the following Y-chromosome specific Invaders: **INV1** (top panel; nuclei in metaphase prior to cell division), **INV2** (second panel; nuclei in interphase), **INV2** (third panel;



inter- and metaphase nuclei), **INV3** (fourth panel; interphase nuclei) and **INV4** (bottom panel; interphase nuclei). Images viewed using Cy3 (left column) or DAPI (middle column) filter settings; overlay images are shown in the right column. Sequences are shown in Table 3. For experimental details, see legend of Figure S9.

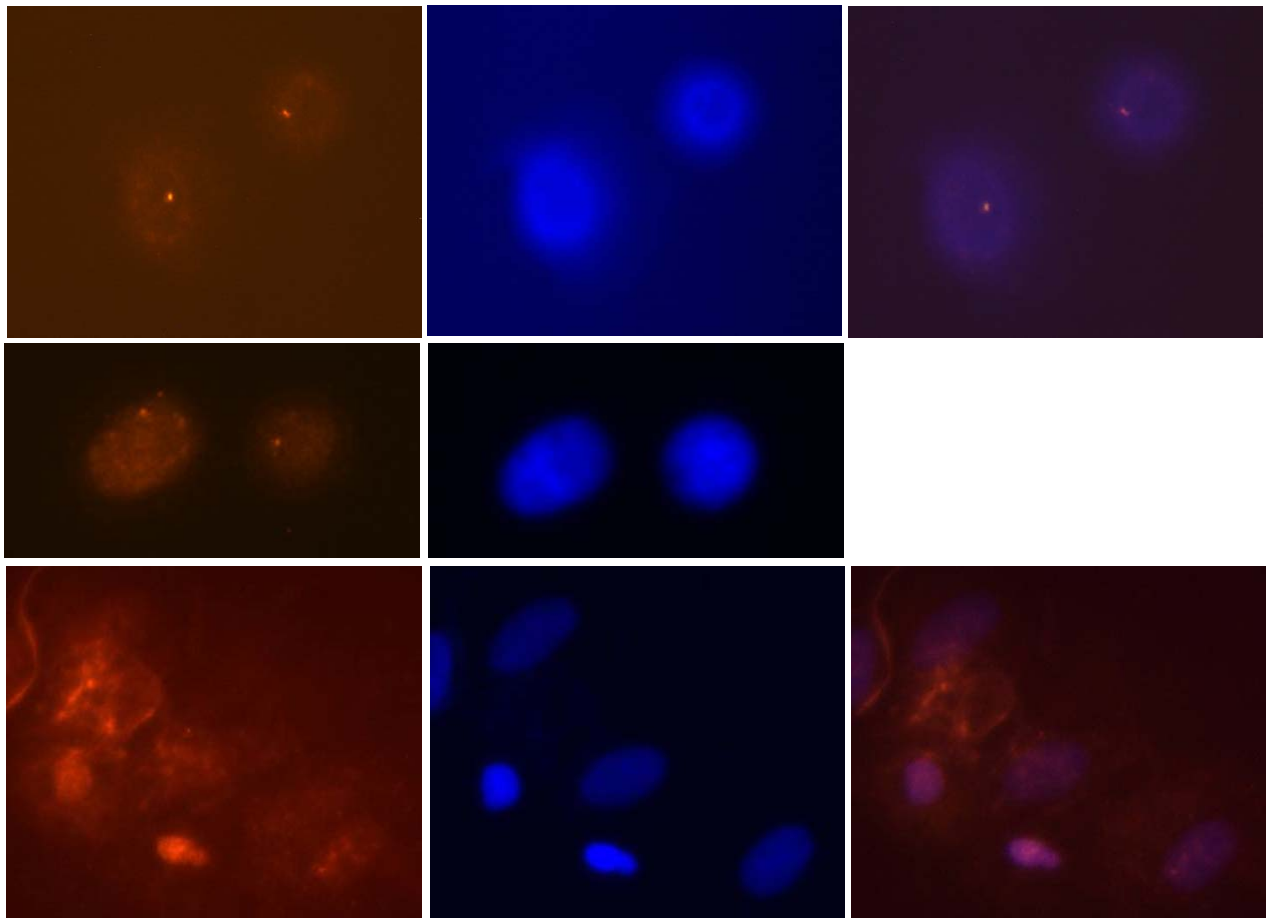


**Figure S11.** Images from FISH experiments involving nuclei from male bovine kidney cells that were treated with proteinase K (upper panel), RNase (middle panel) and DNase (lower panel) prior to incubation with Invader **INV4**. Note the continued presence of Cy3-signals in proteinase K or RNase pre-treated samples, and the absence of Cy3-signals in DNase pre-treated samples. For experimental details, see legend of Figure 9 in the main manuscript.

## REFERENCES

- S1) S. Karmakar, B. A. Anderson, R. L. Rathje, S. Andersen, T. Jensen, P. Nielsen and P. J. Hrdlicka, *J. Org. Chem.*, 2011, **76**, 7119-7131.
- S2) M. A. Morgan, K. Okamoto, J. D. and D. S. English, *Biophys. J.*, 2005, **89**, 2588-2596.
- S3) J. L. Mergny and L. Lacroix, *Oligonucleotides*, 2003, **13**, 515-537.
- S4) B. A. Didion, S. Karmakar, D. C. Guenther, S. P. Sau, J. P. Verstegen and P. J. Hrdlicka, *ChemBioChem*, 2013, **14**, 1534-1538.
- S5) B. Kirkpatrick and R. Monson, *Reprod. Fertil*, 1993, **98**, 335-340.
- S6) S. Karmakar, D. C. Guenther and P. J. Hrdlicka, *J. Org. Chem.*, 2013, **78**, 12040-12048.